PHYSICAL REVIEW B **83**, 121405(R) (2011)

Conductivity of graphene on boron nitride substrates

S. Das Sarma and E. H. Hwang
Condensed Matter Theory Center, Department of Physics, University of Maryland, College Park, Maryland 20742-4111, USA
(Received 7 January 2011; published 15 March 2011)

We calculate theoretically the disorder-limited conductivity of monolayer and bilayer graphene on hexagonal boron nitride (h-BN) substrates, comparing our theoretical results with the recent experimental results. The comparison leads to a direct quantitative estimate of the underlying disorder strength for both short- and long-range disorder in the graphene on the h-BN system. We find that the good interface quality between graphene and h-BN leads to strongly suppressed charged impurity scattering compared with the corresponding SiO_2 substrate case, thus producing very high mobility for the graphene on the h-BN system.

DOI: 10.1103/PhysRevB.83.121405 PACS number(s): 72.80.Vp, 81.05.ue, 72.10.−d, 73.22.Pr

An important recent development in the physics and materials science of graphene[1,2] is the successful fabrication of gated graphene layers on hexagonal boron nitride (h-BN) substrates.[3,4] Since h-BN has the same hexagonal honeycomb lattice structure as graphene itself with an almost matching lattice constant, the expectation has been that graphene on h-BN would have much lower disorder than the generic graphene on SiO_2 substrates, which has almost universally been studied experimentally. This expectation has, in fact, been spectacularly borne out by the recent experiments[3,4] at Columbia University, where both monolayer graphene (MLG) and bilayer graphene (BLG) on h-BN substrates have been shown to have substantially higher (by roughly one order of magnitude or more) carrier mobility than graphene samples on the standard SiO_2 substrates.[1,2] In fact, the quality of graphene on h-BN, as measured by transport experiments, appears to be comparable to that of annealed suspended graphene,[5,6] with both systems exhibiting clear fractional quantum Hall effects attesting to their very high mobility.

In this paper, we consider theoretically electronic transport properties of graphene/BN MLG and BLG systems, using the highly successful Boltzmann-Kubo-RPA formalism, which has earlier been used[1] to study graphene transport on SiO_2 substrates, both for MLG (Refs. 7–9) and BLG (Ref. 10) systems, as well as for the suspended graphene[11] system. Our goal is a thorough quantitative understanding of the specific operational features of resistive scattering mechanisms limiting carrier mobility in graphene on h-BN. By demanding quantitative agreement between our calculated graphene (on h-BN) transport properties with the corresponding experimental data[3,4] for both MLG and BLG systems, we establish the precise role of long-range (e.g., charged Coulomb impurities in the environment) versus short-range (e.g., point defects, neutral scatterers, vacancies) disorder in graphene on h-BN systems. We obtain excellent agreement with the experimental data[3,4] using very reasonable disorder parameters, establishing that the good interface quality between graphene and h-BN (e.g., lack of dangling bonds) leads to strongly suppressed charged impurity scattering compared with the corresponding SiO_2 substrate situation,[7,8] thus providing very high mobility for the graphene on the h-BN system. The relative suppression of long-range scattering compared with the short-range scattering also leads to rather nonlinear-looking MLG conductivity as a function of gate voltage (i.e., carrier density) for graphene on h-BN substrates compared with the SiO_2 substrates; thus, this explains the peculiar experimental finding that the observed BLG (MLG) conductivity on h-BN substrates[3,4] manifests linear (nonlinear) conductivity as a function of the gate voltage. Our theory also naturally explains the weaker observed temperature dependence of MLG conductivity than the BLG conductivity for graphene on the h-BN substrate. The actual conductivity of MLG-BN or BLG-BN (Refs. 3 and 4) is determined by the detailed interplay between the long- and short-range disorder in the relevant system along with the distinct screening properties of the graphene carriers as it is in the usual graphene on SiO_2 substrates.[1,7,8,10,12]

The graphene conductivity σ is given by[1]

$$\sigma = \frac{e^2}{2}\int d\varepsilon\, D(\varepsilon) v_k^2 \tau(\varepsilon)\left(-\frac{\partial f}{\partial \varepsilon}\right), \tag{1}$$

where $f = f(\varepsilon_k)$ is the Fermi distribution function, $D(\varepsilon)$ is the density of states, $v_k = d\varepsilon_k/dk$ is the carrier velocity, and $\tau(\varepsilon)$ is the transport scattering (or relaxation) time, which depends explicitly on the effective disorder scattering potential V:

$$\frac{1}{\tau(\varepsilon)} = \frac{2\pi}{\hbar}\sum_\alpha n_i^{(\alpha)}(z)\int \frac{d^2k'}{(2\pi)^2}\,|V_{\mathbf{k}\mathbf{k}'}(z)|^2\, g(\theta_{\mathbf{k}\mathbf{k}'}) \times (1-\cos\theta_{\mathbf{k}\mathbf{k}'})\delta(\varepsilon_{\mathbf{k}}-\varepsilon_{\mathbf{k}'}), \tag{2}$$

where $\varepsilon_{\mathbf{k}}$ is the graphene carrier energy dispersion for the two-dimensional (2D) wave vector $\mathbf{k}$, z is the position of the impurity, the concentration of which is defined by n_i^α with α denoting the kind of impurity (e.g., long or short range), $g(\theta)$ denotes a known chiral matrix element form factor determined by the band structure (and is therefore different for MLG and BLG), and ($\mathbf{k}$, $\mathbf{k}'$) are the incoming and outgoing carrier 2D wave vector due to the impurity scattering potential $V_{\mathbf{k}\mathbf{k}'}(z)$. Since the details of the transport theory for graphene have been discussed earlier in the literature,[1,7,9,10] we only make a few comments on the calculational aspects of our theoretical results presented in this work: (i) The substrate h-BN is characterized by its static dielectric constant $\kappa_{\rm BN} = 7.0$,[13] leading to an effective background dielectric constant $\kappa = 4.0$, which enters into the definition of the effective disorder potential. (ii) The effective disorder potential V entering Eq. (2) is taken to be the screened disorder, where the screening is by the static graphene (MLG or BLG) dielectric function $\epsilon(q,T)$, which has been calculated earlier in Refs. 14 and 15, respectively, for MLG

and BLG. (iii) We include two types of disorder in our theory, the long-range disorder characterized by randomly distributed charged impurity centers with 2D density of n_i located at the graphene-BN interface and the short-range disorder characterized by an effective strength of $n_d V_0^2$ denoting a white-noise delta-correlated local disorder. (iv) MLG (BLG) 2D energy band dispersion is taken to be linear (quadratic) for our calculations.

The theory is characterized by two parameters n_i and $n_d V_0^2$ describing long- and short-range disorder, respectively. In principle, the effective separation (d) between the location of the charged impurity centers and the 2D graphene layer could also be an additional physically relevant parameter in the transport theory,[1,7,8] but we set $d = 0$ throughout this paper, keeping the number of free parameters to a minimum (only two) and assuming that the random charged impurity centers are located at the graphene-BN interface as consistent with the very high quality of the h-BN crystals used in Refs. 3 and 4. Changing d is equivalent to a readjustment of the unknown charged impurity density n_i and, as such, we can set $d = 0$ without any loss of generality. For obtaining our theoretical transport results, we have varied the parameters n_i and $n_d V_0^2$ arbitrarily over a wide range, obtaining the best regression fit to the high-density data of Refs. 3 and 4 as shown in Figs. 1 and 2.

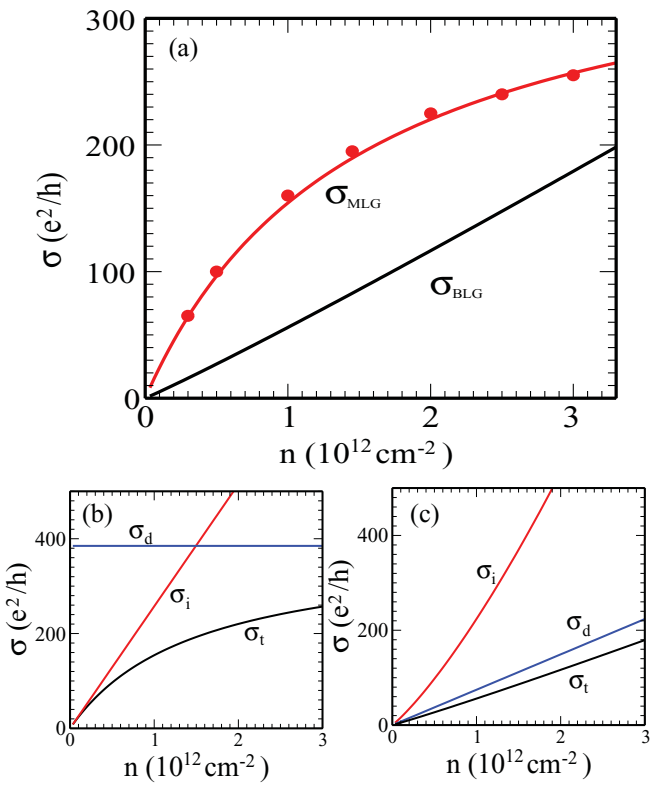

FIG. 1. (Color online) (a) Calculated conductivity of MLG ($\sigma_{\rm MLG}$) and BLG ($\sigma_{\rm BLG}$) using the following parameters: $n_i = 10 \times 10^{10}$ cm^{-2} and $n_d V_0^2 = 0.9$ (eVÅ)^2. Solid dots represent the experimental data points extracted from Ref. 3. In (b) [(c)], we show the individual MLG (BLG) conductivity limited by long-range (σ_i) and short-range scattering (σ_d). σ_t indicates the total conductivity limited by both scatterings.

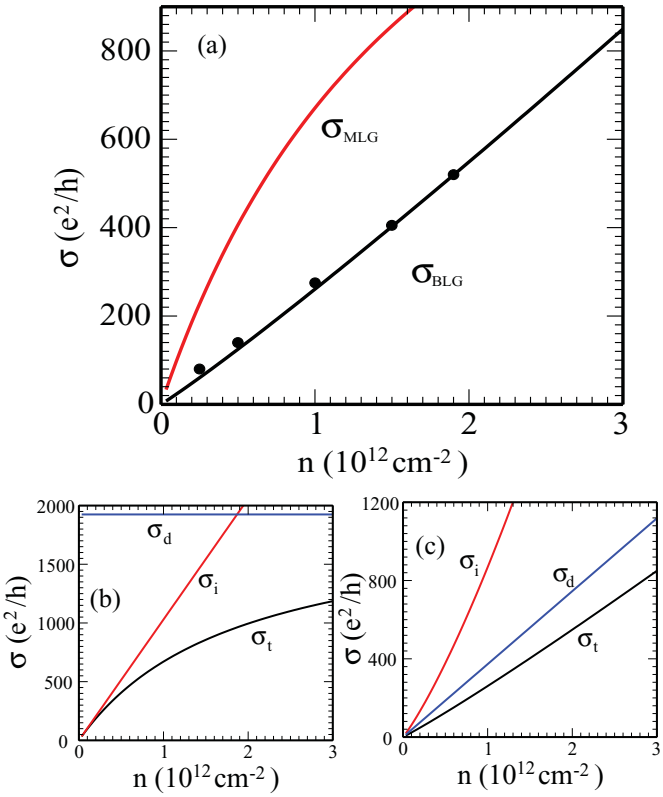

FIG. 2. (Color online) (a) Calculated conductivity of MLG ($\sigma_{\rm MLG}$) and BLG ($\sigma_{\rm BLG}$) using the following parameters: $n_i = 2.5 \times 10^{10}$ cm^{-2} and $n_d V_0^2 = 0.2$ (eVÅ)^2. Solid dots represent the experimental data points extracted from Ref. 3. In (b) [(c)], we show the individual MLG (BLG) conductivity limited by long-range (σ_i) and short-range scattering (σ_d). σ_t indicates the total conductivity limited by both scatterings.

We first show our theoretical results valid at "high" carrier density (n) defined as $n \gtrsim n_i$ away from the minimum conductivity Dirac point regime, where the density fluctuations associated with the inhomogeneous puddle formation can be safely neglected. In Figs. 1 and 2, we show our calculated conductivity (at $T = 0$) $\sigma(n)$ as a function of the carrier density for a few different values of the disorder parameters, choosing the parameters such that we get essentially exact quantitative agreement away from the Dirac point ($n > n_i$) with the experimental data of Ref. 3 for MLG-BN (Fig. 1) and BLG-BN (Fig. 2) systems. In each figure, we present results for both MLG and BLG systems for a fixed set of values of the disorder parameters n_i (long range) and $n_d V_0^2$ (short range) with the results of Fig. 1 (Fig. 2) showing quantitative agreement with the corresponding experimental data for MLG (BLG) on h-BN in Ref. 3. In each figure, we present the individual conductivity limited by long- and short-range scattering as well as the total conductivity compared with the experimental data points extracted from Ref. 3.

Three qualitative features of our theoretical results in Figs. 1 and 2 stand out.

(i) For fixed disorder, MLG conductivity is always larger than BLG conductivity for all densities although they approach each other at very high density as expected.

(ii) The quantitative values of the disorder parameters (i.e., n_i and $n_d V_0^2$) necessary in Figs. 1 and 2 for obtaining agreement with the experimental data[3,4] for graphene on h-BN substrates are typically much smaller (by more than an order of magnitude) than that needed for agreement between theory and experiment with the corresponding graphene on SiO_2 substrates (e.g., Refs. 7 and 8); this is particularly true for the charged impurity density n_i, which has the remarkably small value of $0.3 \times 10^{11} - 1.0 \times 10^{11}$ cm^{-2} for graphene on h-BN substrates compared with $n_i > 10^{12}$ cm^{-2} for graphene on SiO_2 substrates (we note that short-range disorder characterized by $n_d V_0^2$ seems comparable in strength for h-BN and SiO_2 substrates, with h-BN having somewhat smaller values).

(iii) The MLG conductivity results for h-BN substrates are much more sublinear than for the corresponding SiO_2 substrate case, clearly establishing the much weaker role of long-range charged impurity scattering in h-BN systems compared with SiO_2 systems.

It is easy to show theoretically[1,7,8] using Eq. (2) that the charged impurity scattering limited MLG conductivity $\sigma_i^{\rm MLG}$ on h-BN substrates is given approximately by $\sigma_i^{\rm MLG} \approx 25.7(e^2/h)(n/n_i)$, whereas the short-range scattering limited conductivity is given by $\sigma_d^{\rm MLG} \approx 350(e^2/h)/(n_d V_0^2)$, where $n_d V_0^2$ is measured in (eVÅ)^2 units. Our MLG numerical results for long-range scattering shown in Figs. 1 and 2 obey these analytical relations exactly with the net conductivity being given by $\sigma = (\sigma_i^{-1} + \sigma_d^{-1})^{-1}$. For the BLG on h-BN substrates, a simple analytic relation can only be derived for the short-range scattering limited conductivity $\sigma_0^{\rm BLG} = 66.7(e^2/h)(n/n_d V_0^2)$, which is linear in carrier density, with n in units of 10^{12} cm^{-2} and $n_d V_0^2$ in units of (eVÅ)^2. The long-range disorder leads to a $\sigma_i^{\rm BLG} \sim n^{\alpha}$, where $\alpha \approx 1$–1.3 depending on the parameter regime, and no simple analytic relationship can be derived except at very low BLG carrier density where the Coulomb disorder is effectively completely screened out since the BLG screening wave vector becomes much larger than the Fermi wave vector. For this very low carrier density regime ($\ll 10^{12}$ cm^{-2}), the charged impurity disorder-limited BLG conductivity becomes linear in carrier density (i.e., $\alpha = 1$) obeying the approximate relationship $\sigma_i^{\rm BLG} \sim 15(e^2/h)(n/n_i)$. We mention, however, that this formula is not useful for $n < n_i$ since density inhomogeneity effects associated with puddles would dominate close to the charge neutrality point.

The agreement, using reasonable values of disorder parameters, between theoretical results presented in Figs. 1 and 2 with the experimental data[3,4] of the Columbia group indicates that graphene on h-BN indeed has substantially lower long-range Coulomb disorder in its environment than graphene on SiO_2 substrates, most likely due to the high-quality graphene-BN interface without any dangling bonds as already speculated in Ref. 3. A direct consequence of this reduced Coulomb scattering is the manifestly sublinear $\sigma(n)$ observed in the MLG-BN system to be contrasted with the linear $\sigma(n)$ in the MLG-SiO_2 system,[1,7] except at very high densities. We note that our theory indicates a direct way of estimating the strength of both long- and short-range disorder from the high-density MLG-BN $\sigma(n)$ data by obtaining the slope $d\sigma/dn$ at high density (which gives n_i) and by obtaining the intercept of the high density $\sigma(n)$ extrapolated to $n \to 0$, which gives $n_d V_0^2$.

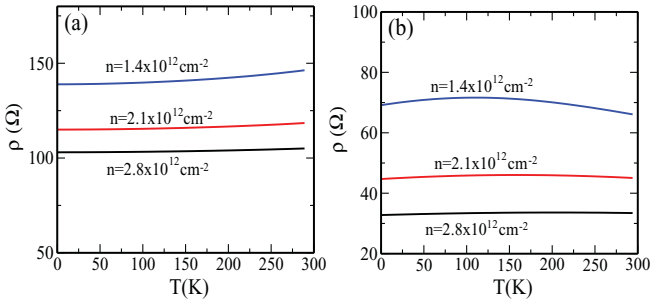

FIG. 3. (Color online) The temperature dependence of the MLG conductivity (a) and the BLG conductivity (b) for several electron densities. In (a) [(b)], the parameters of Fig. 1 (Fig. 2) are used.

In Fig. 3, we present our theoretical results for the temperature dependence of the MLG [Fig. 3(a)] and BLG [Fig. 3(b)] conductivity $\sigma(n,T)$ on h-BN substrates. These results are again valid (similar to those in Figs. 1 and 2) at high carrier density ($n > n_i$) where density inhomogeneity effects are negligible. All phonon effects are neglected here with the temperature dependence arising entirely from the temperature dependence of the screening function and the energy-averaging associated with the finite-temperature smearing of the Fermi surface.[9] The first effect ("screening") produces weak metallic temperature dependence (i.e., σ decreasing with increasing T) since screening weakens at higher temperatures, whereas the second effect ("thermal averaging") produces weak insulating temperature dependence (i.e., σ increasing with increasing T). Although the temperature dependence is weak, as is obvious from Fig. 3, the theoretical behavior of $\sigma(T)$ is qualitatively consistent with the experimental observations[3] away from the Dirac point: (i) MLG manifests weak metallic T dependence, and (ii) BLG manifests weak insulating T dependence. Experimentally, both systems manifest insulating $\sigma(T)$ at the Dirac point where density inhomogeneity effects dominate, but at higher density ($n \gtrsim n_i$), our results are consistent with the experimental findings of Ref. 3.

Finally, we consider in Fig. 4 the low-density transport in graphene-BN systems, where the results (valid for $n \gtrsim n_i$) shown in Figs. 1– 3 do not apply. At low carrier density n ($< n_i$), which is very low ($\sim 10^{10}$ cm^{-2}) for the graphene-BN

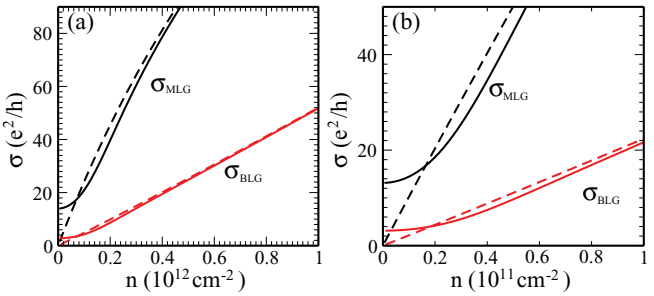

FIG. 4. (Color online) Calculated conductivity using effective medium theory (solid lines) for both MLG ($\sigma_{\rm MLG}$) and ($\sigma_{\rm BLG}$). Dashed lines represent the transport results calculated using Boltzmann transport theory. In (a) and (b), we use the parameters corresponding to Figs. 1 and 2, respectively. Note that the effective medium theory becomes important only at low ($n < n_i$) carrier density where inhomogeneous puddle formation becomes significant.

system because of its extremely weak Coulomb disorder, the graphene layer is known[1,8,16–19] to break up into inhomogeneous puddles due to the failure of screening, and, thus, the naive Boltzmann-Kubo-RPA transport theory, which explicitly assumes a homogeneous carrier density, is no longer valid since the density fluctuations become strong. To demonstrate the effect of puddle formation on graphene-BN transport properties, we have carried out an effective medium theory[10] calculation of transport using $n_{\rm rms} = n_i$, where $n_{\rm rms}$ is the root-mean-square fluctuation in the carrier density due to the puddles induced by the charged impurities. Microscopic self-consistent calculations[10,16] show that $n_{\rm rms} \approx n_i$ is a reasonable qualitative approximation for the density inhomogeneity around the Dirac point. Our $T = 0$ effective medium theory transport results (using the Boltzmann-Kubo-RPA transport formalism) are shown in Fig. 4 for both MLG-BN and BLG-BN systems. The most important features of Fig. 4 are (i) the high-density ($n \gtrsim n_i$) results shown in Figs. 1 and 2 remain valid; and (ii) near the Dirac point (for $n < n_i$), $\sigma(n)$ saturates with a nonuniversal disorder-dependent minimum conductivity,[1,8] the value of which is roughly given by 2–10 (e^2/h), consistent with the experimental observations.[3,4]

We have also carried out an effective medium theory calculation at finite temperature to include the puddle effects on $\sigma(n,T)$. These results (not shown) agree with the results shown in Fig. 3 at high densities ($n > n_i$), but for low carrier densities ($n < n_i$), we qualitatively recover the experimentally observed strongly insulating $\sigma(T)$ induced by the puddles. An important open question is the source of the short-ranged disorder in the system, which may necessitate going beyond the minimal effective model used in our theory requiring *ab initio* calculations.[20]

This work was funded by US-ONR.

[1] S. Das Sarma, S. Adam, E. H. Hwang, and E. Rossi, Rev. Mod. Phys. (to be published).

[2] N. M. R. Peres, Rev. Mod. Phys. **82**, 2673 (2010); A. H. Castro Neto, F. Guinea, N. M. R. Peres, K. S. Novoselov, and A. K. Geim, *ibid*. **81**, 109 (2009).

[3] C. R. Dean, A. F. Young, I. Meric, C. Lee, L. Wang, S. Sorgenfrei, K. Watanabe, T. Taniguchi, P. Kim, K. L. Shepard, and J. Hone, Nat. Nanotechnol. **5**, 722 (2010).

[4] C. R. Dean, A. F. Young, P. Cadden-Zimansky, L. Wang, H. Ren, K. Watanabe, T. Taniguchi, P. Kim, J. Hone, and K. L. Shepard, e-print arXiv:1010.1179.

[5] F. Ghahari, Y. Zhao, P. Cadden-Zimansky, K. Bolotin, and P. Kim, Phys. Rev. Lett. **106**, 046801 (2010).

[6] W. Bao, Z. Zhao, H. Zhang, G. Liu, P. Kratz, L. Jing, J. Velasco, D. Smirnov, and C. N. Lau, Phys. Rev. Lett. **105**, 246601 (2010).

[7] E. H. Hwang, S. Adam, and S. Das Sarma, Phys. Rev. Lett. **98**, 186806 (2007); Y.-W. Tan, Y. Zhang, K. Bolotin, Y. Zhao, S. Adam, E. H. Hwang, S. Das Sarma, H. L. Stormer, and P. Kim, *ibid*. **99**, 246803 (2007).

[8] S. Adam, E. H. Hwang, V. M. Galitski, and S. Das Sarma, Proc. Natl. Acad. Sci. USA **104**, 18392 (2007); J. H. Chen, C. Jang, S. Adam, M. S. Fuhrer, E. D. Williams, and M. Ishigami, Nat. Phys. **4**, 377 (2008).

[9] E. H. Hwang and S. Das Sarma, Phys. Rev. B **79**, 165404 (2009).

[10] S. Das Sarma, E. H. Hwang, and E. Rossi, Phys. Rev. B **81**, 161407 (2010).

[11] K. Bolotin, K. Sikes, Z. Jiang, G. Fudenberg, J. Hone, P. Kim, and H. Stormer, Solid State Commun. **146**, 351 (2008); S. Adam and S. Das Sarma, *ibid*. **146**, 356 (2008).

[12] S. Xiao, J. H. Chen, S. Adam, E. D. Williams, and M. S. Fuhrer, Phys. Rev. B **82**, 041406 (2010).

[13] R. Geick, C. H. Perry, and G. Rupprecht, Phys. Rev. **146**, 543 (1966); P. J. Gielisse, S. S. Mitra, J. N. Plendl, R. D. Griffis, L. C. Mansur, R. Marshall, and E. A. Pascoe, *ibid*. **155**, 1039 (1967).

[14] E. H. Hwang and S. Das Sarma, Phys. Rev. B **75**, 205418 (2007).

[15] E. H. Hwang and S. Das Sarma, Phys. Rev. Lett. **101**, 156802 (2008).

[16] E. Rossi and S. Das Sarma, Phys. Rev. Lett. **101**, 166803 (2008).

[17] J. Martin, N. Akerman, G. Ulbricht, T. Lohmann, J. H. Smet, K. von Klitzing, and A. Yacoby, Nat. Phys. **4**, 144 (2008).

[18] Y. Zhang, V. W. Brar, C. Girit, A. Zettl, and M. F. Crommie, Nat. Phys. **5**, 722 (2009).

[19] A. Deshpande, W. Bao, Z. Zhao, C. N. Lau, and B. J. LeRoy, Appl. Phys. Lett. **95**, 243502 (2009).

[20] J. P. Robinson, H. Schomerus, L. Oroszlany, and V. I. Fal'ko, Phys. Rev. Lett. **101**, 196803 (2008); A. Lherbier, X. Blase, Yann-Michel Niquet, F. Triozon, and S. Roche, *ibid*. **101**, 036808 (2008); S. Yuan, Hans De Raedt, and M. I. Katsnelson, Phys. Rev. B **82**, 115448 (2010).